

Diagnostic Value of Fully Automated Artificial Intelligence Powered Coronary Artery Calcium Scoring from 18F-FDG PET/CT

Claudia Morf

University Hospital Zurich: UniversitatsSpital Zurich

Thomas Sartoretti

University Hospital Zurich: UniversitatsSpital Zurich

Antonio G. Gennari

University Hospital Zurich: UniversitatsSpital Zurich

Alexander Maurer

University Hospital Zurich: UniversitatsSpital Zurich

Stephan Skawran

University Hospital Zurich: UniversitatsSpital Zurich

Andreas A. Giannopoulos

University Hospital Zurich: UniversitatsSpital Zurich

Elisabeth Sartoretti

University Hospital Zurich: UniversitatsSpital Zurich

Moritz Schwyzer

University Hospital Zurich: UniversitatsSpital Zurich

Alessandra Curioni-Fontecedro

University Hospital Zurich: UniversitatsSpital Zurich

Catherine Gebhard

University Hospital Zurich: UniversitatsSpital Zurich

Ronny Buechel

University Hospital Zurich: UniversitatsSpital Zurich

Philipp A. Kaufmann

University Hospital Zurich: UniversitatsSpital Zurich

Martin W. Huellner

University Hospital Zurich: UniversitatsSpital Zurich

Michael Messerli (✉ michael.messerli@usz.ch)

Department of Nuclear Medicine University Hospital Zurich

Keywords: Artificial intelligence, Coronary artery calcium scoring, Coronary artery disease, Deep learning, Positron emission tomography

Posted Date: March 15th, 2022

DOI: <https://doi.org/10.21203/rs.3.rs-1430655/v1>

License:   This work is licensed under a Creative Commons Attribution 4.0 International License. [Read Full License](#)

Abstract

Purpose: To assess the feasibility and accuracy of a fully automated artificial intelligence (AI) powered coronary artery calcium scoring (CACS) method on ungated CT in oncologic patients undergoing 18F-FDG PET/CT.

Materials and Methods: A total of 100 oncologic patients examined between 2007 and 2015 were retrospectively included. All patients underwent 18F-FDG PET/CT and cardiac SPECT myocardial perfusion imaging (MPI) by 99mTc-tetrofosmin within 6 months. CACS was manually performed on non-contrast ECG-gated CT scans obtained from SPECT-MPI (i.e. reference standard). Additionally, CACS was performed fully automatically using a cloud-based, user-independent tool (AI-CACS) on non-contrast, free-breathing, ungated CT scans from 18F-FDG-PET/CT examinations. Agatston scores from the manual CACS and AI-CACS were compared.

Results: On a per-patient basis, the AI-CACS tool achieved a sensitivity and specificity of 85% and 90% for the detection of coronary calcifications. Interscore agreement of CAC scores between manual CACS and AI-CACS was 0.88 (95% CI: 0.827, 0.918). Interclass agreement of risk categories was 0.8 in weighted Kappa analysis with a reclassification rate of 44% and an underestimation of one risk category by AI-CACS in 39% of cases. On a per-vessel basis, interscore agreement of CAC scores ranged from 0.716 (95%CI: 0.605, 0.799) for the circumflex artery to 0.863 (95%CI: 0.803, 0.906) for the left anterior descending artery.

Conclusion: Fully automated AI-CACS as performed on non-contrast free-breathing, ungated CT scans from 18F-FDG-PET/CT examinations is feasible and provides a good estimation of CAC burden. CAC load on ungated CT is, however, generally underestimated by AI-CACS which should be taken into account when considering recommending further diagnostic workup for coronary heart disease.

Introduction

Hybrid 18F-fluorodeoxyglucose positron emission tomography (18F-FDG PET) with computed tomography (CT) has evolved as an important imaging modality for staging and restaging of oncological patients [1]. Clinical 18F-FDG PET/CT examinations consist of a PET scan and a non-contrast, free-breathing, ungated CT. The CT is used for (a) PET attenuation correction but (b) also includes relevant morphological information regarding disease/tumor extent. Even though the appropriate oncological diagnosis and treatment planning is the primary concern in cancer patients, relevant comorbidities should not be underestimated and ideally be described in the imaging report. Indeed, a recent population-based study including more than 3 million cancer patients indicated that the highest number of cardiovascular deaths occurred in the first year following initial cancer [2].

Coronary artery calcium (CAC) is an important biomarker in patients with coronary heart disease (CHD) [3, 4]. Increased CAC scores are strongly associated with cardiovascular mortality and all-cause mortality [3, 4]. 18F-FDG PET/CT examinations are generally not suited for the comprehensive evaluation of CAC or CHD, as the CT scan is neither acquired nor reconstructed with the appropriate scan parameters as recommended for dedicated cardiac CT calcium scans [5–7]. Nonetheless, an opportunistic screening

resulting in the rough estimation of the coronary disease burden by means of CAC would be highly desirable, indeed, this has been recommended in a recent consensus statement of the British Societies of Cardiovascular and Thoracic Imaging [8]. Optimally, this assessment (i.e. CAC scoring, CACS) should be performed fully automatically so that the physician can continue to focus on the oncological workup of the scan. With recent advances in the field of artificial intelligence (AI) for medical imaging [9–12], deep-learning (DL) powered calcium scoring tools have been developed that allow for the quantitative assessment of CAC in a fully automated manner [11–14].

Given the considerations outlined above, these tools would be suited for the opportunistic assessment of CAC in patients undergoing oncologic 18F-FDG PET/CT examinations as quantitative CAC scores are provided without having to perform CAC scoring manually.

In this study, we sought to test the feasibility of such an approach. Specifically, we assessed the quantitative accuracy of an AI-powered CACS tool in estimating CAC from CT scans acquired during oncologic 18F-FDG PET/CT examinations using manual CACS measurements from a dedicated cardiac imaging workup as the standard of reference.

Material And Methods

Study Population

This study was approved by the local ethics committee (BASEC No. 2017 – 01112), and the need for informed consent was waived due to the retrospective nature of the study. The study population was partly shared in previous studies [1, 15]. Our study population was selected from a retrospective cohort study of consecutive patients undergoing (a) a whole-body 18F-FDG-PET/CT for malignant disorders at the University Hospital Zurich between November 2007 and February 2015, and (b) 1-day stress/rest (regadenoson, adenosine, dobutamine, or exercise) myocardial perfusion imaging by 99mTc-tetrofosmin single-photon emission computed tomography (SPECT-MPI) including non-contrast, ECG-gated CT for attenuation correction within 6 months of 18F-FDG-PET/CT imaging to evaluate known or suspected CAD, Fig. 1. CAC scoring was performed manually on the dedicated non-contrast ECG-gated CT scans (120 kV, reconstructed with weighted filtered back projection, a slice thickness of 3 mm and an increment of 1.5 mm) as obtained during myocardial perfusion imaging by two experienced physicians in consensus (i.e. reference standard) using a dedicated software program (Smartscore, GE Healthcare) [16]. Out of the 100 patients, 20 patients were identified with a CAC score of 0, 16 patients with a score of 1–100, 23 patients with a score of 101–400, and 41 patients with a score of >400. An overview of the patient demographics is provided in Table 1.

Table 1
Demographics of study patients ($n = 100$).

Female/male	34 / 66
Age, years	66 ± 11.4 (32–91)
Weight, kg	74.2 ± 16.5 (46.8–140.0)
Height, cm	169.8 ± 9.6 (135–200)
BMI, kg/m ²	25.6 ± 5.2 (17.2–47.3)
Primary Tumor, n (%)	
Head and neck cancer	11%
Lung or pleural cancer	12%
Rectal or colon cancer	13%
Esophageal cancer	20%
Liver tumor	5%
Breast cancer	7%
Pancreatic and biliary cancer	8%
Lymphoma	4%
Others	20%
BMI body mass index, presented as % and mean ± SD (range)	

Whole Body 18F-FDG PET/CT including ungated CT

Patients underwent PET/CT imaging from skull to pelvis one hour after injection of 18F-FDG (including a non-contrast, free-breathing, ungated CT scan). Images were acquired in 3D mode on a Discovery VCT or Discovery RX scanner (GE-Healthcare, Milwaukee, WI, USA). PET/CT and CT images were merged and analyzed using Advantage Window Volume Viewer software (GE-Healthcare, Milwaukee, WI, USA) [1].

Fully automated AI-CAC Scoring

AI-CACS was performed with a fully automated deep-learning based CAC scoring tool (AVIEW CAC, Coreline Soft, access via <https://cloud.corelinesoft.eu/login>). The software was developed based on a 3-dimensional U-net architecture using non-enhanced cardiac CT scans acquired from multiple vendors and scanners. No training data were included in this current study [14, 17]. Initially, the non-contrast, free-breathing, ungated CT scans from the 18F-FDG PET/CT examination were postprocessed in the hospital's PACS system by cropping the image series. Specifically, a second dataset encompassing all images from the lung apex to the lung base was generated for each patient. This anonymized image series was then transferred to the AI tool. Fully automated CACS was then performed without any further user input. The results from CACS were then summarized in a report generated by the AI tool.

Statistical analysis

The data was initially presented with descriptive statistics. Diagnostic accuracy parameters were computed to quantify the AI tools ability to correctly identifying coronary calcium relative to the reference standard. Quantitative CAC scores between the AI tool and the reference standard were compared by means of intraclass correlation coefficient (ICC) analysis, linear regression modelling, and Bland-Altman analysis. Interclass agreement of CAC risk category classes was quantified by means of weighted Kappa analysis. For ICC and weighted Kappa analysis, the following scale was considered for results interpretation: poor (ICC, $k < 0.20$), fair (ICC, $k = 0.21-0.40$), moderate (ICC, $k = 0.41-0.60$), good (ICC, $k = 0.61-0.80$), and excellent (ICC, $k = 0.81-1.00$) agreement [18]. All statistical analyses were performed in the R programming language (<https://www.r-project.org>).

Results

A total of 100 patients who underwent both whole-body 18F-FDG PET/CT and SPECT-MPI (including a dedicated ECG-gated CACS) within a 6-month period scan were enrolled. In all patients, the AI-CACS tool successfully managed to process the dataset (i.e. ungated low dose CT).

Diagnostic accuracy of AI-CACS for the detection of coronary calcifications

The sensitivity of the AI-CACS tool for the detection of coronary calcifications analysed per-patient was 85.0%, and analysed per-coronary artery analysis 74.5% (left main, LM), 82.0% (left anterior descending, LAD), 64.2% (left circumflexus, LCX), and 61.7% (right coronary artery, RCA), respectively. Further results of the per-patient and per-coronary artery diagnostic performance of AI-CACS are presented in Table 2.

Table 2

Diagnostic performance of AI-CACS with manual CACS as reference. Data are shown per patient and per coronary artery.

	Per patient	Per coronary artery			
	All patients	LM	LAD	RCX	RCA
Sensitivity	85.0% (77.2–92.8%)	74.5% (62.5–86.5%)	82.0% (73.4–91.0%)	64.2% (51.2–77.1%)	61.7% (49.4–74.0%)
Specificity	90.0% (76.9–100%)	79.6% (68.3–90.9%)	100% (100–100%)	95.7% (90.0–100%)	95.0% (88.2–100%)
Diagnostic accuracy	86.0% (77.6–92.1%)	77.0% (67.5–84.8%)	87.0% (78.8–92.9%)	79.0% (69.7–86.5%)	75.0% (65.3–83.1%)
PPV	97.1% (93.2–100%)	79.2% (67.7–90.7%)	100% (100–100%)	94.4% (87.0–100%)	94.9% (88.0–100%)
NPV	60.0% (42.5–77.5%)	75.0% (63.2–86.8%)	67.5% (53.0–82.0%)	70.3% (59.1–81.5%)	62.3% (50.1–74.4%)
Total, n	100	100	100	100	100
True positive, n	68	38	60	34	37
False negative, n	12	13	13	19	23
True negative, n	18	39	27	45	38
False positive, n	2	10	0	2	2
LM left main, LAD left anterior descending, RCX ramus circumflex, RCA right coronary artery, PPV positive predictive value, NPV negative predictive value					
Data are presented as sensitivity, specificity, diagnostic accuracy, PPV, NPV % (95% confidence interval).					

Quantitative agreement of AI-CACS with manual CACS

Interscore agreement (i.e. ICC) of CAC scores between the AI tool and manual measurements as the reference standard was 0.88 (95% CI: 0.827, 0.918). The linear regression model between CAC scores of the AI tool and the reference standard (Fig. 2) revealed an R^2 of 0.84, an intercept of 180, and a slope of 1.2. Bland-Altman analysis showed a bias of 274.8, a lower and upper limit agreement of -714.9 and 1264.5, respectively, see Fig. 2. On a per-vessel basis, interscore agreement was 0.761 (95% CI: 0.664, 0.831) for

LM, 0.863 (95% CI: 0.803, 0.906) for LAD, 0.716 (95% CI: 0.605, 0.799) for CX and 0.812 (95% CI: 0.733, 0.869) for RCA.

In terms of risk category classes (Table 3), a weighted Kappa score of 0.800 was found for the interclass agreement between the AI tool and the reference standard. Reclassification of risk category occurred in 44 cases (44%), of which shifting by one category in 39 cases (89%) and by two categories in 5 cases (11%). In 42 cases (42%), the AI tool underestimated the risk category, while in 2 cases (2%), the AI tool overestimated the CAC burden (risk class 1 instead of risk class 0).

Table 3

Confusion matrices of risk categories between AI-CACS and manual CACS. Weighted kappa values were 0.8.

Manual CACS	AI-CACS				Total	Underestimation ^a	Overestimation ^a	Concordance ^a
	0	1–100	101–400	> 400				
0	18	2	0	0	20	-	2 (10.0%)	18 (90.0%)
1-100	11	5	0	0	16	11 (68.8%)	0	5 (31.2%)
101–400	1	17	5	0	23	18 (78.3%)	0	5 (21.7%)
> 400	0	4	9	28	41	13 (31.7%)	-	28 (68.3%)
CACS coronary artery calcium scoring								
^a i.e. manual coronary artery calcium scoring as reference								

Representative cases of the AI-CACS tool correctly identifying the coronary calcium burden in a patient are presented in Fig. 3. Further examples presenting false negative findings as well as the two patients of the study cohort that were falsely classified to have an Agatston Score > 0 (i.e. false positive findings) are presented in Fig. 4 and Fig. 5, respectively.

Discussion

In this retrospective study, we aimed to assess the value of a fully automated AI tool to accurately quantify CAC in patients undergoing non-contrast free-breathing ungated CT as part of an oncologic 18F-FDG PET/CT examination.

Our data indicate, that the AI tool manages to detect and quantify CAC with relatively high accuracy without requiring any user input. However, AI-CACS from ungated CT generally underestimates CAC burden, which should be kept in mind if further diagnostic workup for CAD are considered to recommend. Nonetheless, this study further provides evidence that CAC scores can be extracted effortlessly from various types of CT scans, thus potentially expanding the diagnostic value and impact of a given examination.

Following a recent consensus statement from the British societies of cardiovascular imaging/cardiac computed tomography and thoracic imaging, physicians are urged to report incidental coronary calcifications on all CT scans covering the chest as CAC is an important marker of CAD in both symptomatic and asymptomatic patients [8]. Specifically, CAC is associated with a poorer prognosis in various patient groups, including cancer patients. Notably, a sub-analysis of the National Lung Screening Trial showed that CAC scores of > 100 were associated with a four to sevenfold increase in mortality risk as compared to patients without CAC [19]. For CAC grading, the authors recommend using a semi-quantitative ordinal scoring system instead of the conventional quantitative Agatston scoring system. While the authors acknowledge that the Agatston scoring system represents the gold standard assessment for CAC, they point out that the additional time effort, and use of dedicated software may prevent physicians from implementing and performing CACS on non-dedicated CT scans, as in the case of PET/CT imaging [8].

In the current study, we present a viable approach that enables physicians to extract quantitative Agatston scores from ungated CT scans as acquired for attenuation correction of oncologic PET scans. This AI tool runs fully automatically without any further user input and generates a detailed CACS report that can directly be sent to the user or to the institutions' PACS. Notably, the tool has previously been validated by Vonder et al., who tested the tools' performance relative to manual CACS measurements in a cohort of 997 patients who had undergone a dedicated cardiac CT protocol including calcium scans as part of a cardiovascular screening program. The authors found an interscore agreement of 0.958 and an interclass agreement of 0.96 for risk categories thus confirming the AI tools ability to perform CACS accurately on dedicated cardiac calcium CT scans [14].

In contrast, we found an interscore agreement of 0.88 and an interclass agreement of 0.800 for risk categories. In this regard, it should be noted that dedicated calcium scans are performed in breath-hold and with ECG-gating. This is not the case for the CT acquired during PET/CT examinations and may therefore significantly impact CAC quantification accuracy. Specifically, it has been shown that the calcium load can be underestimated on ungated CT scans [20–23]. Furthermore, it should be noted that the acquisition and reconstruction parameters of the CT scan from PET/CT imaging may differ from those recommended for a dedicated cardiac calcium scan. For example, the latter should be performed at 120 kV and should be reconstructed with weighted filtered back projection [5, 7].

Despite these differences and challenges, our AI tool achieved a good performance in detecting and quantifying CAC. Specifically, while reclassification of risk categories frequently occurred (44% of cases), risk categories nearly always only (i.e., 89%) shifted by two category. Furthermore, in nearly all cases, the risk category was underestimated by the AI tool, which may partially be owed to the inherent limitations of an ungated CT scan for CAC detection. This should be kept in mind nonetheless, so recommendation for further workup of potential CAD when using AI-CACS on CT scans from PET/CT scans should rather generously be made by physicians.

Lastly, we would like to emphasize that we did not further optimize the AI tool prior to study onset by performing any specific or further training on our dataset. Thus, the data used in the current study

represents a true validation set. In this regard it, should be noted that the performance of the AI tool may be further improved in the future by training the algorithm with further study/institution specific data.

Our study has the following limitations: First, this was a retrospective single-center study with a limited number of subjects. Importantly it should be acknowledged that the results inherently depend on the examined patient cohort. Here, we used a unique and heterogeneous patient cohort of oncologic patients with scans ranging back to 2007. Incidentally, the AI tool may provide even better results when using more recent scans and scans from a more homogenous patient cohort (performed on more modern scanners). Second, we did not perform manual CACS on the CT scans from PET/CT imaging. This would have allowed us to better quantify the measurement inaccuracy of the AI tool itself. This should be investigated in future studies. Third, as a reference standard, we used manual CACS scores from a dedicated cardiac SPECT-MPI examination performed within 6 months of the oncologic PET/CT. CAC scores are not expected to change within this time frame, nevertheless, it should be acknowledged that minor changes may have occurred, thus potentially introducing a bias.

In conclusion, our study indicates that an AI tool allows for the fully automatic extraction of CAC scores from ungated CT scans as acquired in patients undergoing oncologic 18F-FDG PET/CT. This allows physicians to extract CAC scores effortlessly from oncologic 18F-FDG PET/CT examinations, thus enabling an opportunistic screening of CAD and allowing for the further expansion of the diagnostic spectrum and value of the imaging modality.

Abbreviations

AI = Artificial intelligence

CAC = Coronary artery calcium

CACS = Coronary artery calcium scoring

CHD = Coronary heart disease

CT = Computed tomography

DL = Deep-learning

F18-FDG = F18-Fluorodeoxyglucose

MPI = Myocardial perfusion imaging

PET = Positron emission tomography

SPECT = Single-photon emission computed tomography

SUV_{max} = Maximum standardized uptake value

Declarations

Acknowledgements

Dr. Stephan Skawran is supported by a grant from the Palatin-Foundation, Switzerland. Dr. Michael Messerli received a research grant from the Iten-Kohaut Foundation, Switzerland. Dr. Michael Messerli, Dr. Antonio G. Gennari and Dr. Huellner are supported by a grant from the CRPP "AI Oncological Imaging Network of the University of Zurich".

Dr. Michael Messerli would like to thank Prof. G. K. von Schulthess for his invaluable support of this work.

Funding:

Dr. Martin W. Huellner received grants from GE Healthcare and a fund by the Alfred and Annemarie von Sick legacy for translational and clinical cardiac and oncological research.

Competing interests

The University Hospital of Zurich holds a research agreement with GE healthcare (unrelated to current study). Other than that, the authors declare that they have no competing interests.

Availability of data and materials

The datasets used and/or analyzed during the current study are available from the corresponding author on reasonable request.

Ethics approval and consent to participate

All procedures performed in studies involving human participants were in accordance with the ethical standards of the institutional and/or national research committee and with the 1964 Helsinki Declaration and its later amendments or comparable ethical standards. This retrospective study protocol was approved by the local institutional ethics committee and written informed consent for the scientific use of medical data was obtained from all patients.

Consent for publication

Not applicable.

References

1. Haider A, Bengs S, Schade K, et al. Myocardial 18F-FDG Uptake Pattern for Cardiovascular Risk Stratification in Patients Undergoing Oncologic PET/CT. JCM. 2020;9:2279. <https://doi.org/10.3390/jcm9072279>.

2. Sturgeon KM, Deng L, Bluethmann SM, et al. A population-based study of cardiovascular disease mortality risk in US cancer patients. *Eur Heart J*. 2019;40:3889–97. <https://doi.org/10.1093/eurheartj/ehz766>.
3. Peng AW, Dardari ZA, Blumenthal RS, et al. Very High Coronary Artery Calcium (≥ 1000) and Association With Cardiovascular Disease Events, Non-Cardiovascular Disease Outcomes, and Mortality: Results From MESA. *Circulation*. 2021;143:1571–83. <https://doi.org/10.1161/CIRCULATIONAHA.120.050545>.
4. Clerc OF, Fuchs TA, Stehli J, et al. Non-invasive screening for coronary artery disease in asymptomatic diabetic patients: a systematic review and meta-analysis of randomised controlled trials. *Eur Heart J - Cardiovasc Imaging*. 2018;19:838–46. <https://doi.org/10.1093/ehjci/jey014>.
5. McCollough CH, Ulzheimer S, Halliburton SS, et al. Coronary Artery Calcium: A Multi-institutional, Multimanufacturer International Standard for Quantification at Cardiac CT. *Radiology*. 2007;243:527–38. <https://doi.org/10.1148/radiol.2432050808>.
6. Messerli M, Rengier F, Desbiolles L, et al. Impact of Advanced Modeled Iterative Reconstruction on Coronary Artery Calcium Quantification. *Acad Radiol*. 2016;23:1506–12. <https://doi.org/10.1016/j.acra.2016.08.008>.
7. Gebhard C, Fiechter M, Fuchs TA, et al. Coronary artery calcium scoring: Influence of adaptive statistical iterative reconstruction using 64-MDCT. *Int J Cardiol*. 2013;167:2932–7. <https://doi.org/10.1016/j.ijcard.2012.08.003>.
8. Williams MC, Abbas A, Turr E, et al. Reporting incidental coronary, aortic valve and cardiac calcification on non-gated thoracic computed tomography, a consensus statement from the BSCI/BSCCT and BSTI. *BJR*. 2021;94:20200894. <https://doi.org/10.1259/bjr.20200894>.
9. Schwyzer M, Martini K, Benz DC, et al. Artificial intelligence for detecting small FDG-positive lung nodules in digital PET/CT: impact of image reconstructions on diagnostic performance. *Eur Radiol*. 2020;30:2031–40. <https://doi.org/10.1007/s00330-019-06498-w>.
10. van Griethuysen JJM, Fedorov A, Parmar C, et al. Computational Radiomics System to Decode the Radiographic Phenotype. *Cancer Res*. 2017;77:e104–7. <https://doi.org/10.1158/0008-5472.CAN-17-0339>.
11. Winkel DJ, Suryanarayana VR, Ali AM, et al (2021) Deep learning for vessel-specific coronary artery calcium scoring: validation on a multi-centre dataset. *Eur Heart J - Cardiovasc Imaging* jeab119. <https://doi.org/10.1093/ehjci/jeab119>.
12. Eng D, Chute C, Khandwala N, et al. Automated coronary calcium scoring using deep learning with multicenter external validation. *npj Digit Med*. 2021;4:88. <https://doi.org/10.1038/s41746-021-00460-1>.
13. van Velzen SGM, Lessmann N, Velthuis BK, et al. Deep Learning for Automatic Calcium Scoring in CT: Validation Using Multiple Cardiac CT and Chest CT Protocols. *Radiology*. 2020;295:66–79. <https://doi.org/10.1148/radiol.2020191621>.
14. Vonder M, Zheng S, Dorrius MD, et al (2021) Deep Learning for Automatic Calcium Scoring in Population-Based Cardiovascular Screening. *JACC: Cardiovascular Imaging* S1936878X21005660.

<https://doi.org/10.1016/j.jcmg.2021.07.012>.

15. Fiechter M, Roggo A, Burger IA, et al. Association between resting amygdalar activity and abnormal cardiac function in women and men: a retrospective cohort study. *Eur Heart J - Cardiovasc Imaging*. 2019;20:625–32. <https://doi.org/10.1093/ehjci/jez047>.
16. Gräni C, Vontobel J, Benz DC, et al. Ultra-low-dose coronary artery calcium scoring using novel scoring thresholds for low tube voltage protocols—a pilot study. *Eur Heart J - Cardiovasc Imaging*. 2018;19:1362–71. <https://doi.org/10.1093/ehjci/jey019>.
17. Lee J-G, Kim H, Kang H, et al. Fully Automatic Coronary Calcium Score Software Empowered by Artificial Intelligence Technology: Validation Study Using Three CT Cohorts. *Korean J Radiol*. 2021;22:1764. <https://doi.org/10.3348/kjr.2021.0148>.
18. Landis JR, Koch GG. The measurement of observer agreement for categorical data. *Biometrics*. 1977;33:159–74.
19. Chiles C, Duan F, Gladish GW, et al. Association of Coronary Artery Calcification and Mortality in the National Lung Screening Trial: A Comparison of Three Scoring Methods. *Radiology*. 2015;276:82–90. <https://doi.org/10.1148/radiol.15142062>.
20. Takx RAP, de Jong PA, Leiner T, et al. Automated Coronary Artery Calcification Scoring in Non-Gated Chest CT: Agreement and Reliability. *PLoS ONE*. 2014;9:e91239. <https://doi.org/10.1371/journal.pone.0091239>.
21. Mylonas I, Kazmi M, Fuller L, et al. Measuring coronary artery calcification using positron emission tomography-computed tomography attenuation correction images. *Eur Heart J - Cardiovasc Imaging*. 2012;13:786–92. <https://doi.org/10.1093/ehjci/jes079>.
22. Xia C, Vonder M, Pelgrim GJ, et al. High-pitch dual-source CT for coronary artery calcium scoring: A head-to-head comparison of non-triggered chest versus triggered cardiac acquisition. *J Cardiovasc Comput Tomogr*. 2021;15:65–72. <https://doi.org/10.1016/j.jcct.2020.04.013>.
23. Fan R, Shi X, Qian Y, et al. Optimized categorization algorithm of coronary artery calcification score on non-gated chest low-dose CT screening using iterative model reconstruction technique. *Clin Imaging*. 2018;52:287–91. <https://doi.org/10.1016/j.clinimag.2018.08.015>.

Figures

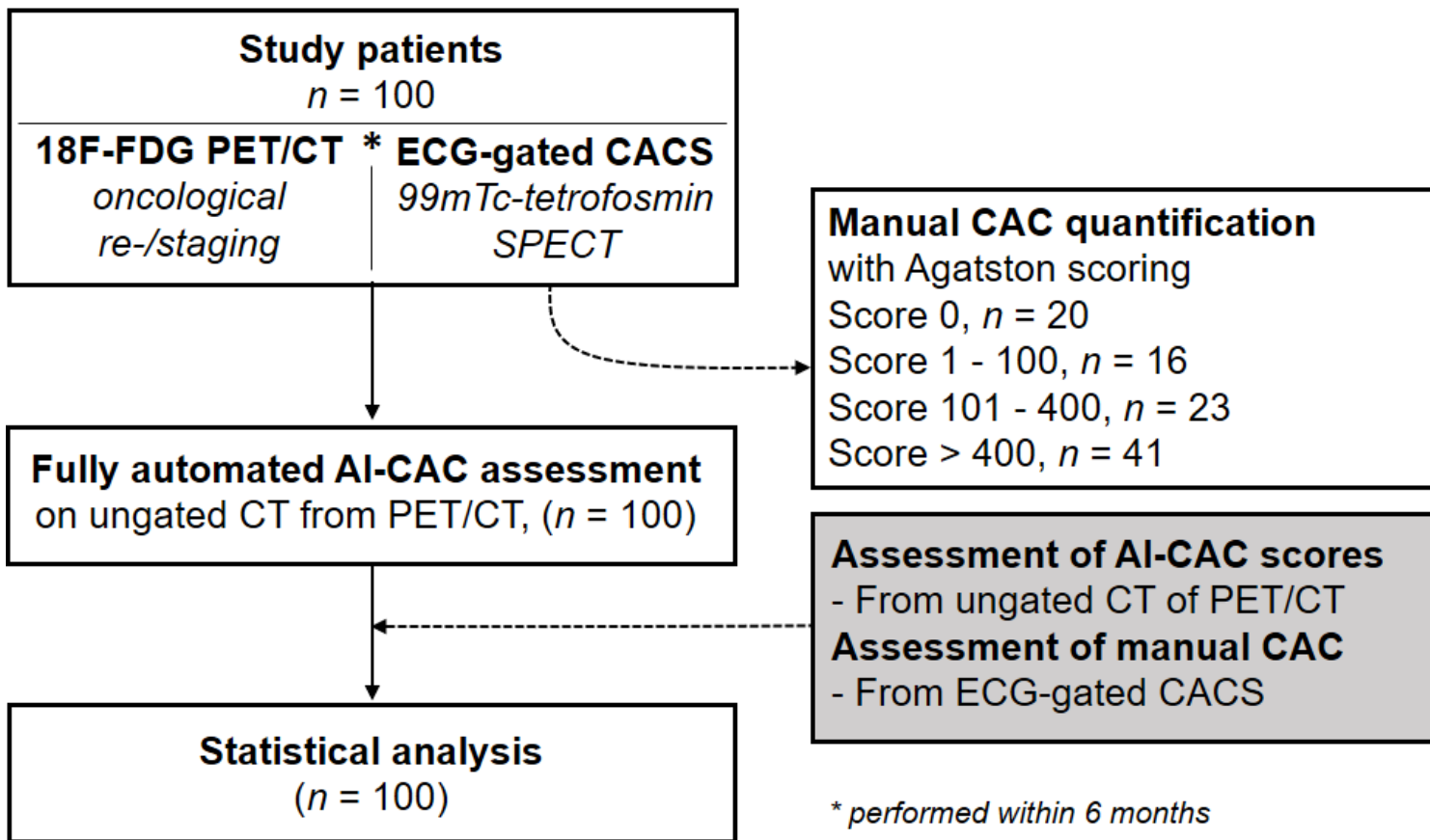


Figure 1

Flow chart of study.

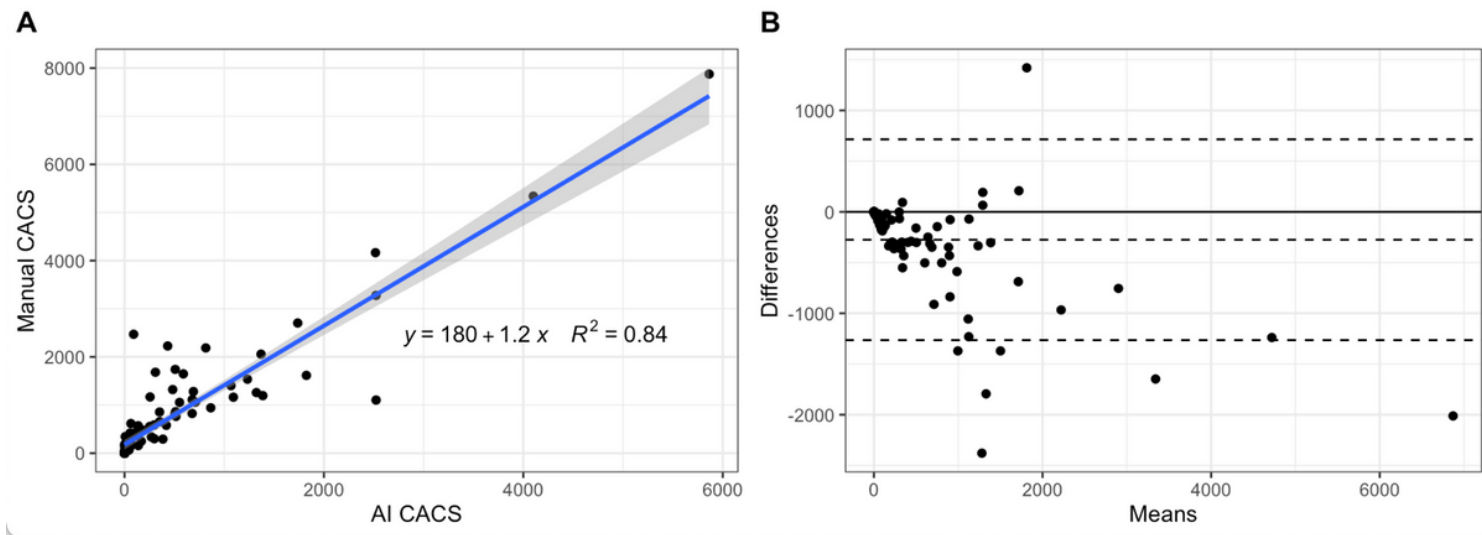


Figure 2

Scatter plot depicting a linear regression model between CAC scores from AI-CACS and manual CACS as well as Bland-Altman plot showing the relationship between CAC scores from AI-CACS and manual CACS.

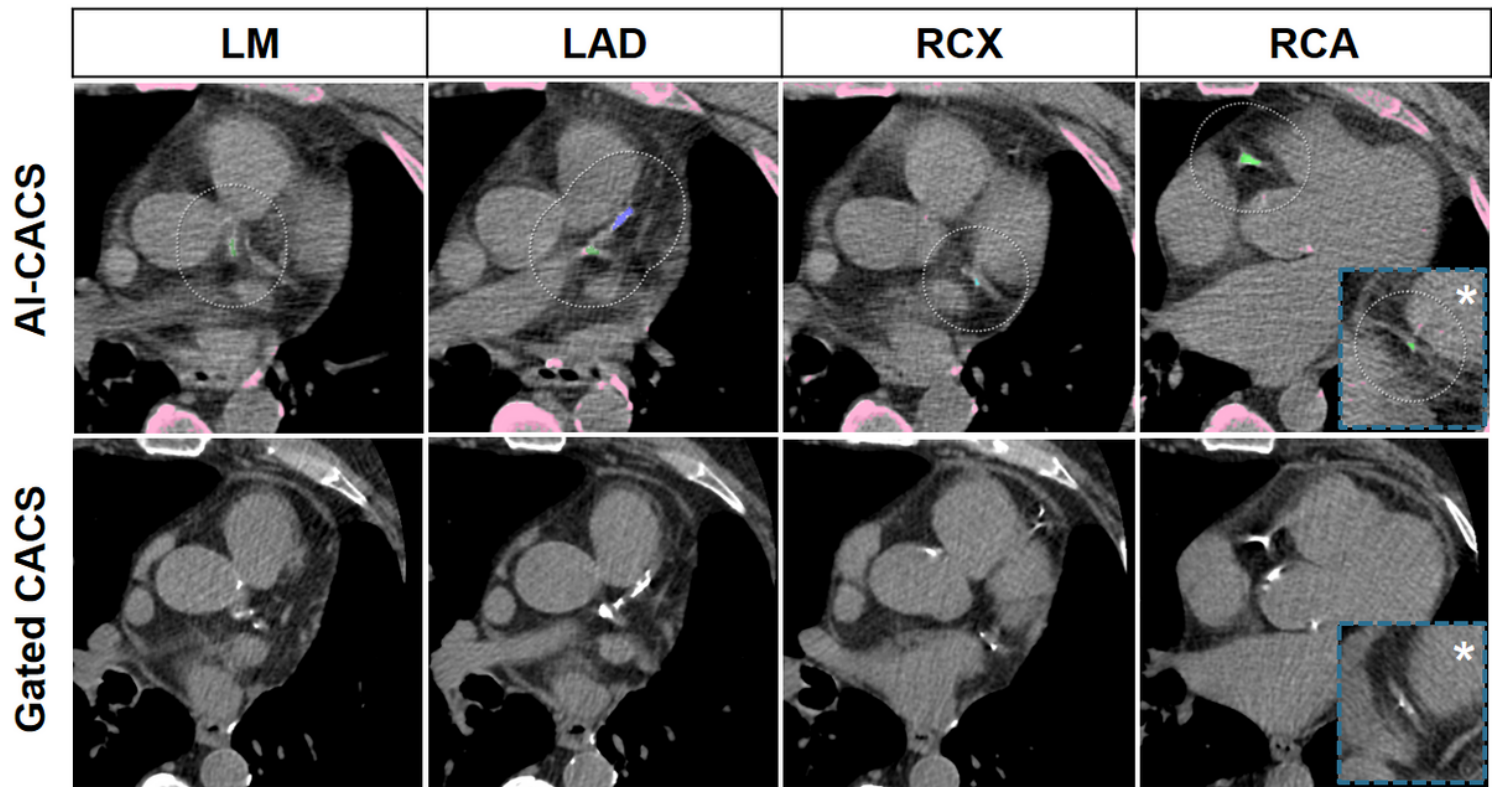


Figure 3

Representative CT images of a 69-year-old man with a body mass index of 26.3 kg/m² with severe coronary artery calcifications. Images from ungated CT from a PET/CT performed for restaging of a rectal adenocarcinoma are presented in the upper row and dedicated gated CAC CT from myocardial perfusion single photon emission computed tomography performed 99 days later are presented in the lower row. Coronary calcifications in the left main (LM), left anterior descending (LAD), ramus circumflexus (RCX), and right coronary artery (RCA) including the distal segment (asterisk), were correctly marked by the AI-CACS tool resulting in a score of 865. The score from dedicated CAC scan was 942.



Figure 4

Representative false negative markings from the AI-CACS tool on un gated CT from PET/CT in a 73-year-old man undergoing PET/CT. Dedicated gated coronary calcium scan showed small coronary calcifications in the right coronary artery (A) and left anterior descending as well as left circumflex artery (B). However the calcifications are not depicted on un gated low dose PET/CT (C and D) performed for staging of lung cancer.

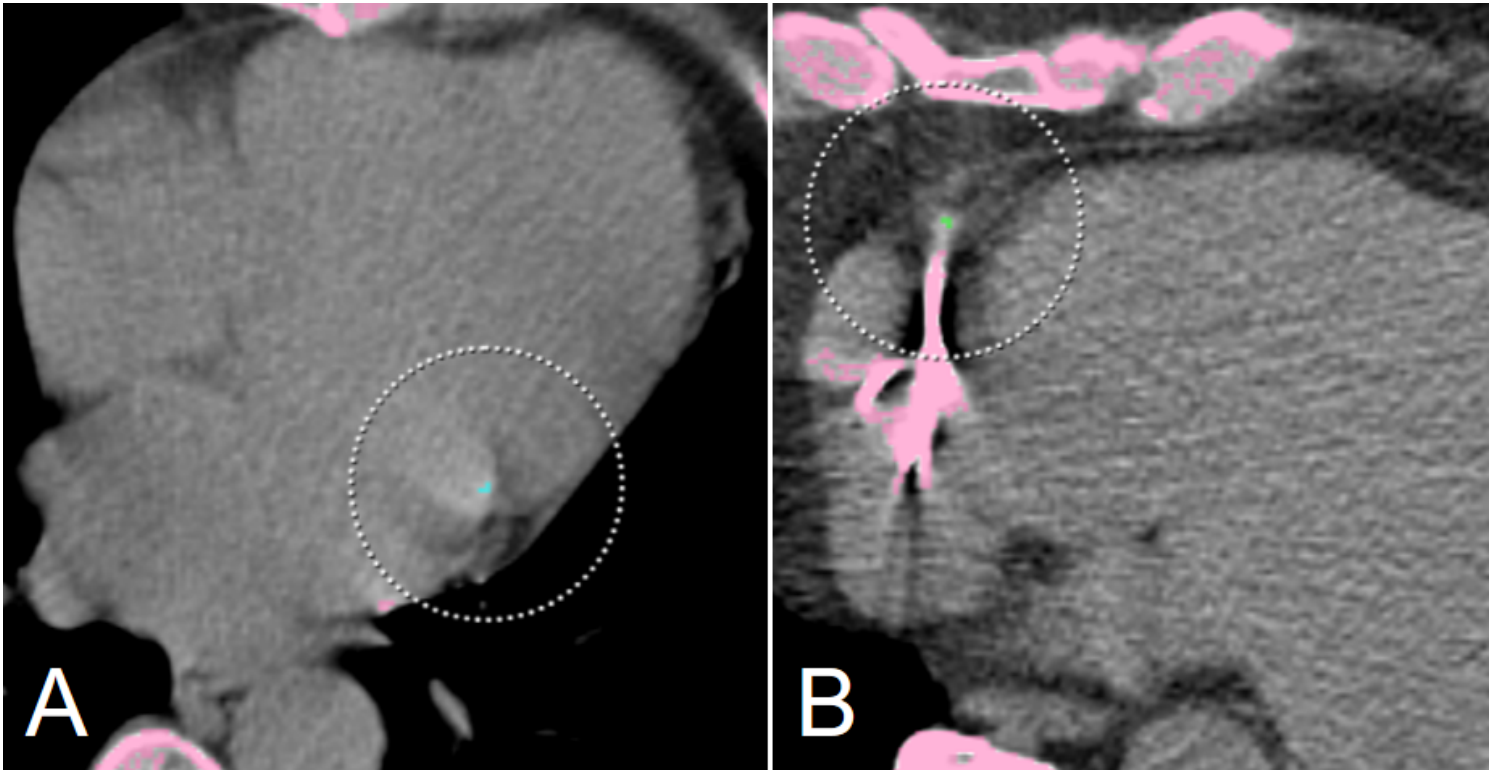


Figure 5

Two representative false-positive ratings from the AI-CACS tool on ungated CT from PET/CT. No coronary calcifications are present in a 66-year-old woman undergoing PET/CT for staging of gastric cancer (A), however small calcifications of mitral valve were falsely marked as ramus circumflexus CAC. In another 66-year-old male patient (B) no CAC was found in dedicated gated CAC scan, however small areas of increased density due to image noise adjacent to a pacemaker electrode were marked as calcification.